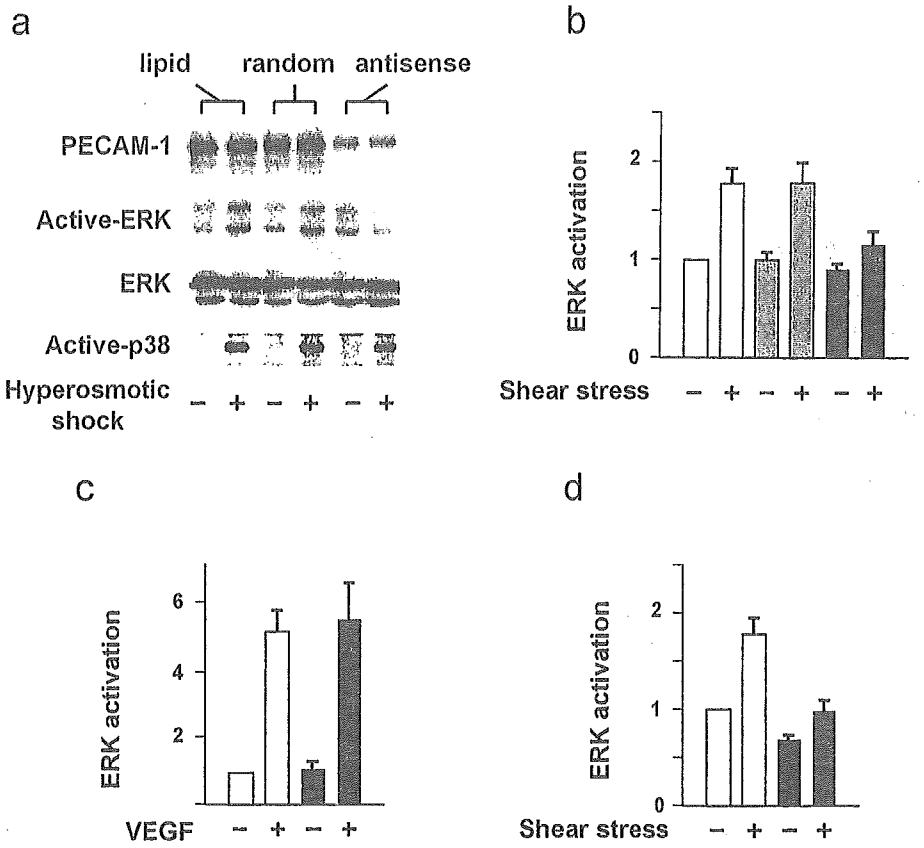

Fig. 2 Crucial requirements of PECAM-1 tyrosine phosphorylation and SHP2 phosphatase activity for flow-induced ERK activation in endothelial cells. (a) Bovine aortic endothelial cells (BAECs) were treated with PECAM-1 antisense S-oligo (antisense), scrambled S-oligo (random), or lipid carrier (lipid). Cells were grown to confluence and treated with (+) or without (−) hyperosmotic shock (+300 mM sucrose) for 10 min. Cell lysates were immunoblotted with antibodies indicated in the figure. (b) FLAG-ERK2 was coexpressed with HA-PECAM-1 cytoplasmic domain (filled bar), with Y663F/Y686F mutations (shaded bar), or vector only (blank bar) in BAECs. Confluent transfectants were exposed to laminar flow with fluid shear stress of 15 dyn/cm^2 (+) or below 1 dyn/cm^2 (−) for 10 min. Cell lysates were immunoprecipitating with anti-FLAG followed by immunoblotting with anti-active ERK. Relative levels of active FLAG-ERK2 are shown. The wild type PECAM-1 cytoplasmic domain, but not the Y/F mutant, showed a dominant negative effect. (c) HA-PECAM-1 cytoplasmic domain did not inhibit ERK activation by VEGF (50 ng/ml, 10 min). (d) FLAG-ERK2 was coexpressed with a phosphatase-inactive mutant of SHP2 (filled bar) or vector alone (blank bar). Overexpression of phosphatase-inactive SHP2 inhibited the flow-induced ERK activation.

SHP2の離脱というサイクルが回っており，常に低レベルの情報発信がなされているのではないかと考えている．流れ刺激はこのサイクルを活性化し有意な情報を伝えるのではないだろうか．

5. 引っ張り力に応答するPECAM-1

内皮細胞にはPECAM-1のチロシンリン酸化を介した流れ刺激のシグナル伝達機構があることはほぼ確実といえるが，PECAM-1の役割はどのようなものであろうか．シグナル増幅器として機能しているのか，あるいはセンサーの構成要素となっているのだろうか．この疑問に明確に答えることは容易ではないが，我々はPECAM-1に直接外力を加えることで回答に接近しようとしている．そもそものきっかけになった実験はわれわれにとって危機的なものであった．普通，培養内皮細胞は敷石状の単層になったものを使用する．生体内の内皮層のモデルとして考えるからである．隙間だらけの培養内皮を使って同じような実験をしてみたところ，PECAM-1のチロシンリン酸化はほとん

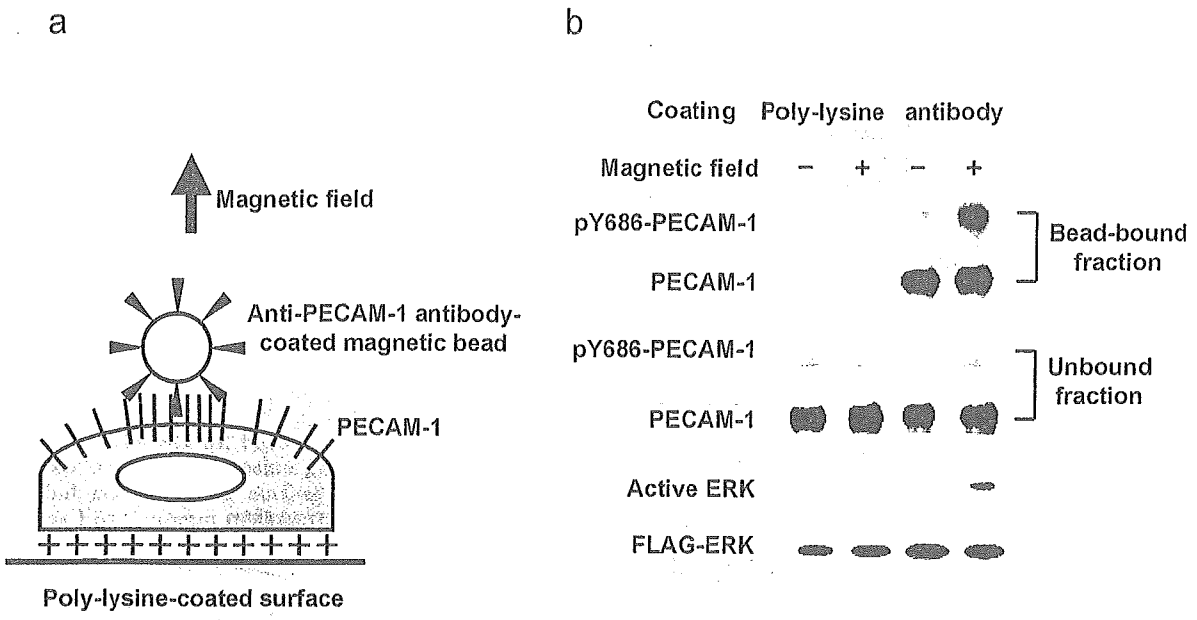

Fig. 3 PECAM-1 tyrosine phosphorylation and ERK activation by direct application of mechanical force to PECAM-1. (a) A scheme for the experiment. Bacteriological dishes were coated sequentially with poly-lysine and heat-inactivated BSA. BAECs plated sparsely on the coated-surface were cultured for 1 h in serum-free medium. BAECs transiently expressing FLAG-ERK2 were used in some experiments. Magnetic beads coated with anti-PECAM-1 extracellular domain (loops 1-2) or poly-lysine were allowed to adhere to the cell surface for 20 min and a strong static magnetic field was applied for 10 min. (b) The bead-bound fraction was collected from the cell lysate. The bound fraction and the remaining cell lysate (unbound fraction) were immunoblotted with anti-pY686-PECAM-1 and reprobed with anti-PECAM-1. The lysates were also immunoprecipitated by anti-FLAG and immunoblotted with anti-active ERK. PECAM-1 bound to the anti-PECAM-1 beads was tyrosine phosphorylated in a magnetic-field dependent manner. ERK activation occurred in BAECs whose PECAM-1 was tugged by the antibody-coated beads.

ど起こらないのにERKの活性化がみられた．アンチセンスオリゴでPECAM-1発現を抑制してもERKの活性化には影響がなく，このような条件ではPECAM-1を介さない流れ刺激応答があることが分かった．おそらく他の研究グループから報告されているインテグリンを介したシグナル伝達と考えられる(16)．その後の研究で，PECAM-1が働くためにはPECAM-1がエンゲージしていることが必須であることが明らかになってきた．逆に，敷石状の単層構造をとっている内皮細胞ではPECAM-1非依存性のERK活性化は無視できる程度になっている．また，以前からPECAM-1のチロシンリン酸化はアクチン細胞骨格を破壊すると強く抑制されることが分かっていた(17)．これらのことはPECAM-1がセンサーの役割を果たしていることを示唆するものと考えられた．

そこで，PECAM-1分子を直接引っ張ることを試みた(Fig. 3)．ホモフィリックな結合を担っているループ1-2に対する特異抗体を作製し，磁気ビーズ表面に結合した．内皮細胞をポリリジン処理した表面に低密度で接着させ，インテグリンもPECAM-1もエンゲージできない状態を作った．インテグリンやPECAM-1は細胞表面全体に拡散して分布するようになり，確かに高浸透圧処理してもERKの活性化は見られない．このような内皮細胞に抗体ビーズを付着させると，PECAM-1はビーズの周囲に集積する．ビーズを強力な静磁場で引っ張るとビーズに結合しているPECAM-1はチロシンリン酸化し，ERKの活性化が起きた(11)．抗体の代わりにポリリジンを共有結合させたビーズを用いると，ビーズは細胞膜に接着し，磁場をかけると細胞膜を引っ張るのにもかかわらず，PECAM-1のリン酸化もERKの活性化も検出できない．ポリリジンビーズにはPECAM-1は結合しない．この結果は，細胞膜の変形がPECAM-1を引っ張るように働いた時にのみPECAM-1を介したERKの活性化が起こることを示し，

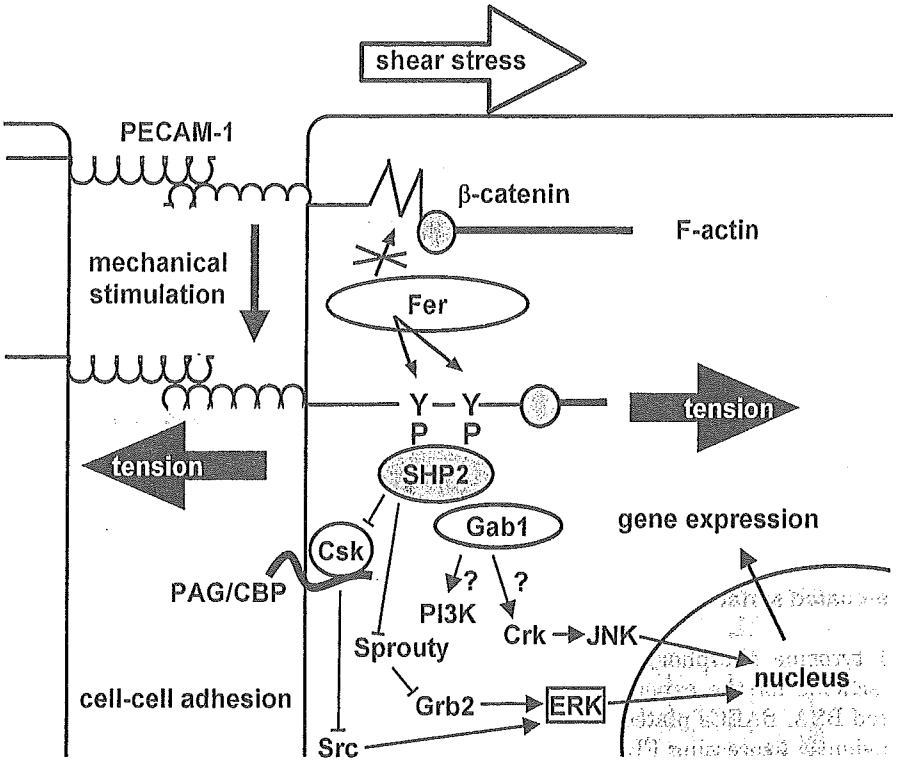

Fig. 4 A model for mechanosignal transduction by PECAM-1. The model depicts the following scenario. When an endothelial cell is under no mechanical stress, PECAM-1 is in a closed state in which Y663 and Y686 are unavailable to kinase. When mechanical force acts on PECAM-1, it is converted to an open state in which the tyrosine residues can be phosphorylated, presumably by Fer. SHP2 and Gab1 are recruited to phosphorylated PECAM-1 and trigger a signaling cascade leading to ERK activation.

PECAM-1 がセンサーあるいはセンサー複合体の構成要素となっていることを示唆する．

6. 流れセンシングの分子メカニズム

流れの力学作用を検出するためには，結局のところ，シアストレスにより直接，あるいは細胞変形を介して間接的に，ある分子がコンフォメーション変化を起こし，それが細胞内の化学的情報に転換されているはずだということになる．つまり，センシングのメカニズムを明らかにするということは，力学的作用でコンフォメーション変化を起こす分子あるいは分子集合体を特定し，その変化が化学的情報に転換される仕組みを明らかにすることに他ならない．こうした視点からこれまで紹介した実験結果を最も単純に説明するモデルが Fig. 4 である．PECAM-1 は外側で相手側の PECAM-1 と結合し，細胞内では何らかの分子を介してアクチン繊維と結合している．PECAM-1 の細胞内ドメインは折りたたまれており，BTAM の 2 つのチロシン残基はリン酸化されにくい状態にある．細胞変形により PECAM-1 が引っ張られると，細胞内ドメインは開き，チロシンキナーゼがアクセス可能になり，シグナル伝達が始まる．実際には折りたたまれた状態と開いた状態が熱平衡にあり，この平衡が PECAM-1 分子にかかる張力で変化するのであろう．

PECAM-1 の生理的チロシンリン酸化酵素が何であるのかは謎であったが，最近，Fer キナーゼがその有力候補であることを見出した(18)．Fer は Fes/Fps と共に特異なファミリーをなす非受容体形チロシンキナーゼであり，SH3 ドメインを持たない代わりに，FCH ドメインを持ち，細胞間や細胞基質間の接着制御に関与している(19)．Fer によるチロシンリン酸化で注目されるのは Y663 と Y686 をリン酸化することである．これまでに報告された Src や Csk は Y686 リン酸化酵素であり，SHP2 の活性化に対する寄与の大きい Y663 はリン酸化しない(20)．Fer は活性化機構を含めてまだ良くわかっていないキナーゼであり，

流れセンシングにおけるFerの役割を明らかにする過程でこのモデルがさらに進化し，センシングの分子メカニズムを明らかにできることを期待したい．

追記：本研究の大半は増田と大澤正輝博士(現Duke大学)，藤原敬己博士（現Rochester大学）が中心になって行ったものである．本総説の当該部分の内容に関する責任は全て増田にある．

文　献

1) 増田道隆　藤原敬己．シアストレス．血管と内皮．1999;9:669-678.
2) Harada N, Masuda M, Fujiwara K. Fluid flow and osmotic stress induced tyrosine phosphorylation of an endothelial cell 128 kDa surface glycoprotein. Biochem Biophys Res Commun. 1995;214:69-74.
3) Osawa M, Masuda M, Harada N, Lopes RB, Fujiwara K. Tyrosine phosphorylation of platelet endothelial cell adhesion molecule-1 (PECAM-1, CD31) in mechanically stimulated vascular endothelial cells. Eur J Cell Biol. 1997;72:229-237.
4) Newman PJ. The biology of PECAM-1. J Clin Invest. 1997;99:3-8.
5) Newman PJ. Switched at birth: a new family for PECAM-1. J Clin Invest. 1999;103:5-9.
6) Masuda M, Osawa M, Shigematsu H, Harada N, Fujiwara K. Platelet endothelial cell adhesion molecule-1 is a major SH-PTP2 binding protein in vascular endothelial cells. FEBS Lett. 1997;408:331-336.
7) Ilan N, Cheung L, Miller S, Mohsenin A, Tucker A, Madri JA. Pecam-1 is a modulator of stat family member phosphorylation and localization: lessons from a transgenic mouse. Dev Biol. 2001;232:219-232.
8) Pellegatta F, Chierchia SL, Zocchi MR. Functional association of platelet endothelial cell adhesion molecule-1 and phosphoinositide 3-kinase in human neutrophils. J Biol Chem. 1998;273:27768-27771.
9) Ilan N, Cheung L, Pinter E, Madri JA. Platelet-endothelial cell adhesion molecule-1 (CD31), a scaffolding molecule for selected catenin family members whose binding is mediated by different tyrosine and serine/threonine phosphorylation. J Biol Chem. 2000;275:21435-21443.
10) Newman PJ, Newman DK. Signal transduction pathways mediated by PECAM-1. New roles for an old molecule in platelet and vascular biology. Arterioscler Thromb Vasc Biol. 2003;23:953-964.
11) Osawa M, Masuda M, Kusano K, Fujiwara K. Evidence for a role of platelet endothelial cell adhesion molecule-1 in endothelial cell mechanosignal transduction: is it a mechanoresponsive molecule? J Cell Biol. 2002;158:773-785.
12) Zhang SQ, Yang W, Kontaridis MI, Bivona TG, Wen G, Araki T, et al. Shp2 regulates SRC family kinase activity and Ras/Erk activation by controlling Csk recruitment. Mol Cell. 2004;13:341-355.
13) Kim HJ, Bar-Sagi D. Modulation of signalling by Sprouty: a developing story. Nat Rev Mol Cell Biol. 2004;5:441-450.
14) Hanafusa H, Torii S, Yasunaga T, Matsumoto K, Nishida E. Shp2, an SH2-containing protein-tyrosine phosphatase, positively regulates receptor tyrosine kinase signaling by dephosphorylating and inactivating the inhibitor Sprouty. J Biol Chem. 2004;279:22992-22995.
15) Gu H, Neel BG. The 'Gab' in signal transduction. Trends Cell Biol. 2003;13:122-130.
16) Chen KD, Li YS, Kim M, Li S, Yuan S, Chien S, Shyy JY. Mechanotransduction in response to shear stress. Roles of receptor tyrosine kinases, integrins and Shc. J Biol Chem. 1999;274:18393-18400.
17) Masuda M, Osawa M, Shigematsu N, Harada N, Lopes RB, Kusano K, et al. Platelet endothelial cell adhesion molecule-1 (CD31) is involved in mechano-signal transduction in endothelial cells. In: Oda Y, editor. Cell volume regulation: the molecular mechanism and volume sensing machinery. Amsterdam: Elsevier Science Publishing Co Inc; 1998. p.23-33.
18) Kogata N, Masuda M, Kamioka Y, Yamagishi A, Endo A, Okada M, et al. Identification of Fer tyrosine kinase localized on microtubules as a platelet endothelial cell adhesion molecule-1 phosphorylating kinase in vascular endothelial cells. Mol Biol Cell. 2003;14:3553-3564.
19) Greer P. Closing in on the biological functions of Fps/Fes and Fer. Nat Rev Mol Cell Biol. 2002;3:278-289.
20) Cao MY, Huber M, Beauchemin N, Famiglietti J, Albelda SM, Veillette A. Regulation of mouse PECAM-1 tyrosine phosphorylation by the Src and Csk families of protein-tyrosine kinases. J Biol Chem. 1998;273:15765-15772.

日本臨牀　第64巻・第2号（平成18年2月号）別刷

特集：ナノテクノロジーと医療

ナノレベルイメージングによる分子構造と機能の解析

盛　英三　　望月直樹　　武田壮一
井上裕康　　中村　俊　　土屋利江

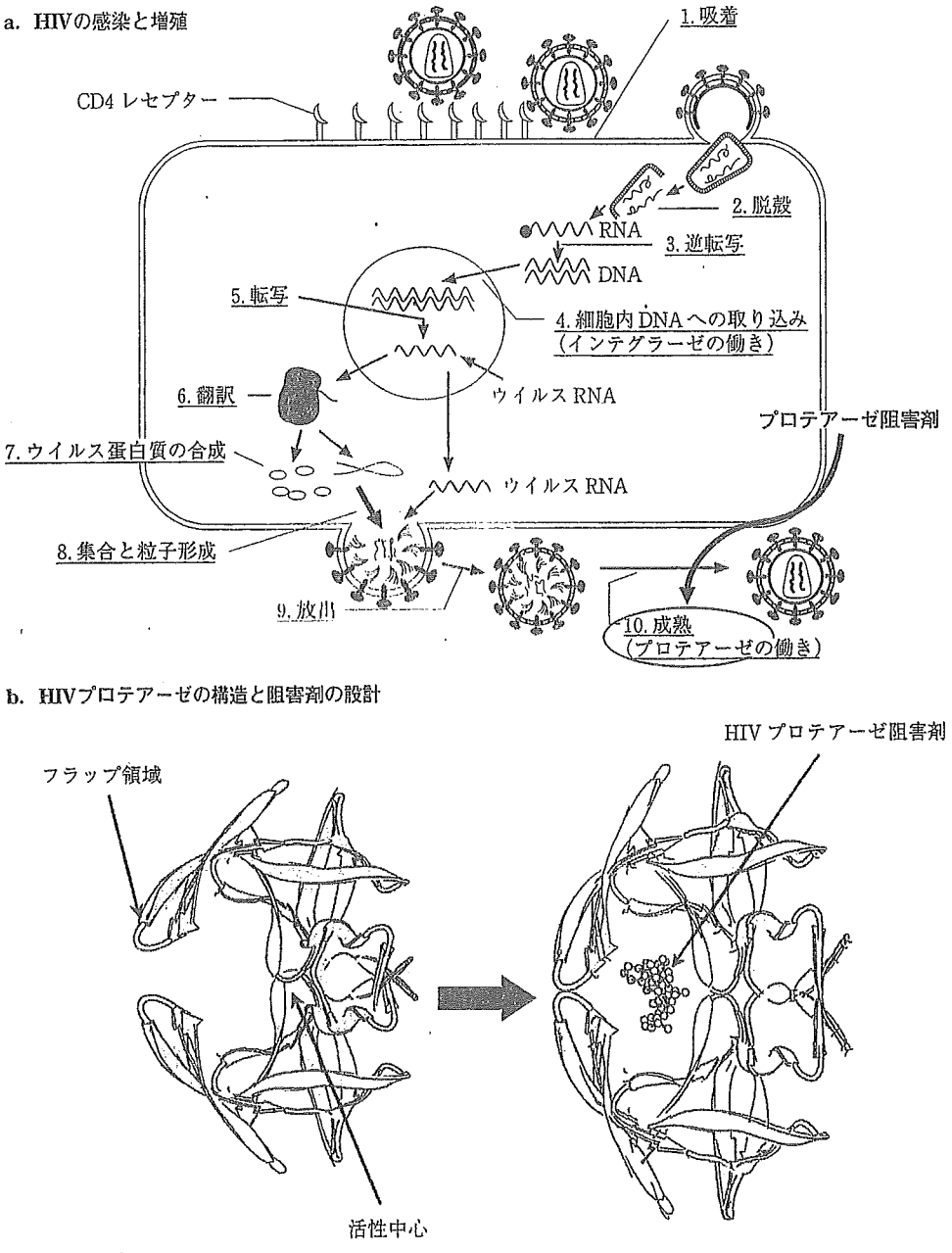

図1 AIDSウイルスの増殖過程と蛋白構造に基づくHIVプロテアーゼ阻害薬の作用機構

テアーゼ阻害薬), 白血病治療薬(グリベック)について以下に述べる.

AIDSウイルス, HIVは活性化外殻蛋白gp120によりCD4陽性Tリンパ球に感染し, 自己増殖をする. その際自己由来のプロテアーゼによって前駆体蛋白から活性化外殻蛋白を得る(図1-a). このHIVプロテアーゼの構造に基づいて設計され, その活性中心を選択的に阻害する目的で設計された薬剤がHIVプロテアーゼ阻害薬である(図1-b). 本剤はAIDSの発症を遅らせることに貢献した[1].

慢性骨髄性白血病ではフィラデルフィア染色

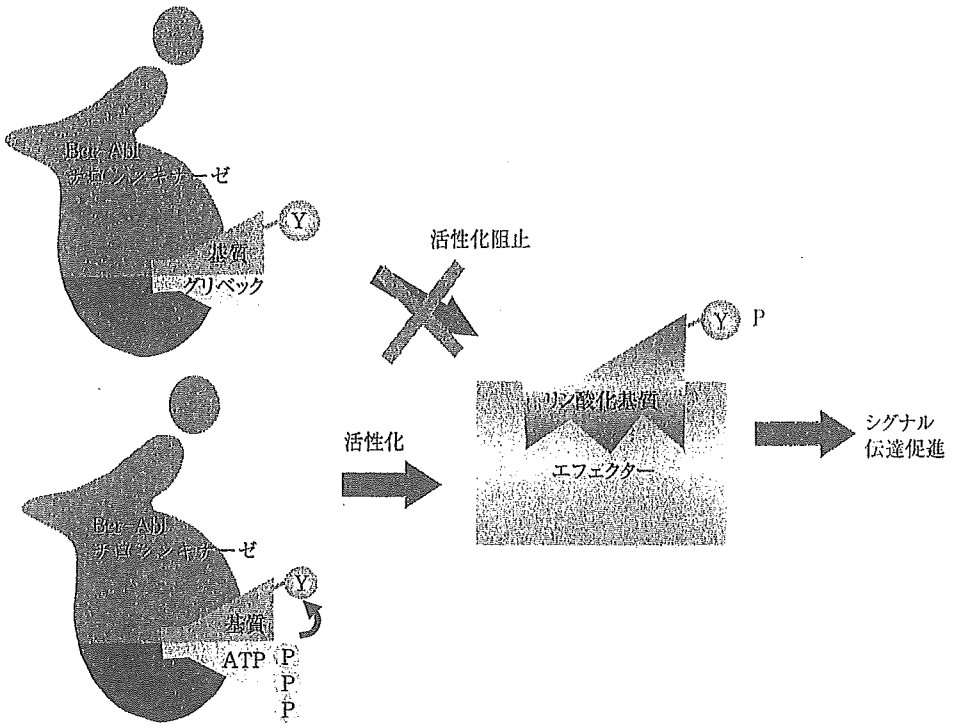

図2 慢性白血病治療薬(グリベック)の蛋白構造に基づく作用機構

体に由来するBcr-Ablチロシンキナーゼが恒常的な増殖シグナル伝達系の活性化を通じて慢性骨髄性白血病発症の原因になると考えられている．同酵素はATPと基質に結合し，ATPから切り離したリン酸基で基質のチロシン残基をリン酸化する．グリベックはBcr-AblチロシンキナーゼのATP結合部位の詳細な構造に基づいて設計され，基質のチロシンリン酸化を構造特異的に阻害して白血病化を防ぐ(図2)[2]．

このような構造に基づいて薬剤設計を行うことで標的蛋白との結合の特異性を高め，副作用を減少させることを期待できる．

2. ヒト心筋トロポニンの構造解析とそれに基づく創薬の可能性

心筋収縮を調節する心筋トロポニンの中核部分(コアドメイン)の構造は分担研究者である武田と理化学研究所の前田らによって解析され，Nature誌に報告された(Vol 424, 2003)[3]．前田らの総説[4]に基づき，トロポニンの筋収縮調節メカニズムについて述べる．

筋収縮はアクチンとミオシンの滑り運動による．アクチンフィラメントはアクチン，トロポニン，トロポミオシンを含む複合体であり，それらの3分子は7：1：1の存在比をもつ．トロポニンの存在下でアクチンとミオシンはカルシウムイオン濃度に応じた収縮と弛緩を行う．

図3に心筋トロポニンのコアドメインの構造を示す．トロポニンはTnC，TnI，TnTと呼ばれる3つのポリペプチド鎖からなる．これまでの研究により，TnIは収縮抑制因子，TnCは脱抑制因子，TnTはTnCの脱抑制を弱める因子(カルシウム濃度依存性の付加因子)であることが示されている[5]．

トロポニンのコアドメインは更に調節頭部とITアームの2つのサブドメインに分かれる．調節頭部はカルシウムイオンとの結合を通じてトロポニンの構造変化とそれに基づくアクチンとミオシンの滑り運動に対するスイッチの役割を果たす．ITアームは剛性を有するコイルドコイ

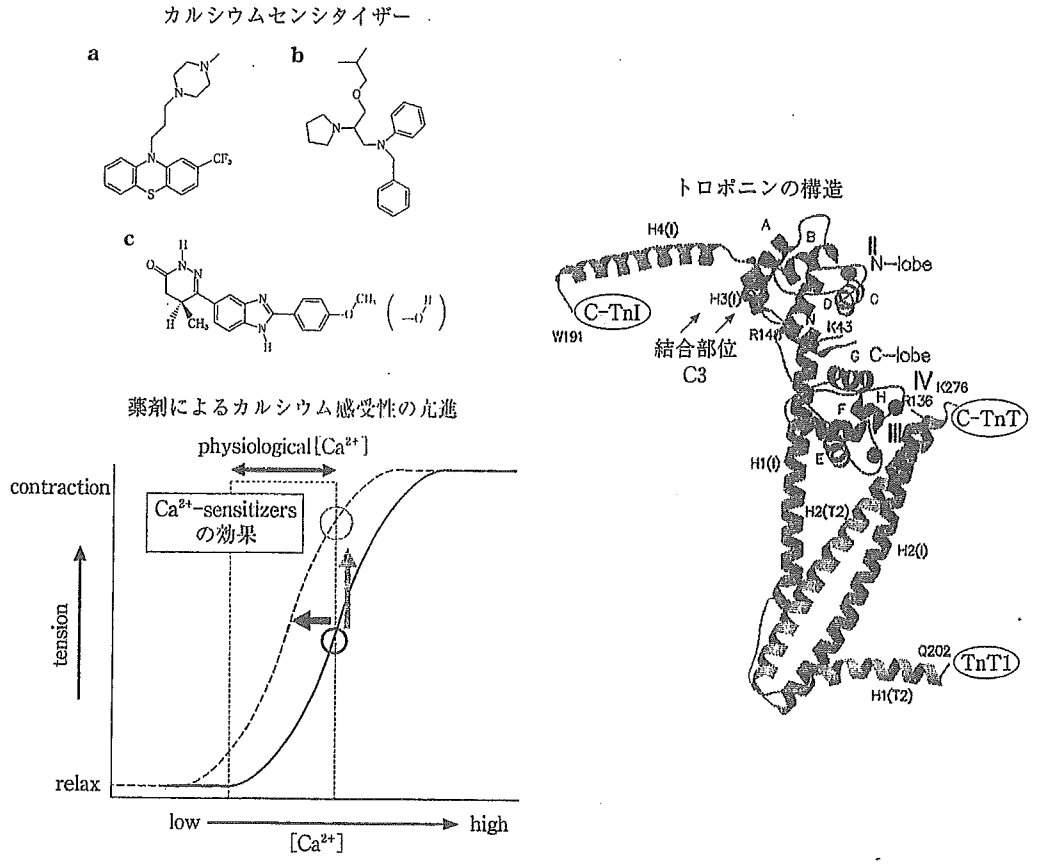

図3　トロポニンコアドメインの構造(文献[3]より改変引用)

ル構造からなる．TnCはN末端側とC末端側の2つの球状部がαヘリックスで連結された構造をもつ．カルシウム濃度にかかわらずC末側球状部はTnIに結合し，TnCをトロポニン分子内に常につなぎとめている．一方，TnCのN末端側球状部は細胞内カルシウム濃度が上昇した場合のみ構造が開き，TnIの第二結合部位(両親媒性αヘリックスH3)を結合する．これにより，TnIの調節領域全体がトロポミオシン/アクチンより解離し，アクチンとミオシンの滑り運動が始まる．

TnCのN末端側球状部にカルシウムセンシタイザーが結合すると，同球状部は開いた構造をとりTnIの第二結合部位を結合しやすくなる．すなわち，TnCによるTnIの脱抑制が起こりやすくなる．前述のようにTnTはTnCの脱抑制作用にカルシウム濃度依存性を付加することができるので，TnCとTnTの制御を組み合わせることで段階的な筋収縮の増強を実現できるかもしれない．近年循環器領域では血管作動性薬剤で優れた新薬が数多く開発されてきたが，ジギタリス以来，これを超える強心剤が生まれていない．従来の強心剤は細胞内カルシウムイオン濃度を高めて強心作用を誘導するために，細胞に対する負荷(カルシウム overload)が不可避であった．1980年代後半に開発されたカルシウムセンシタイザーと呼ばれた薬剤群はカルシウムイオン濃度-張力関係を左方にシフトさせることにより，低い細胞内カルシウムイオン濃度で高い収縮力を得ることができる理想的な強心剤ではないかと期待された[6]．しかしながら，これらの薬剤の臨床使用経験から，短期的に心筋収縮力は高まるものの，心不全患者の長期予後の改善に役立つことはなかった．これらのカ

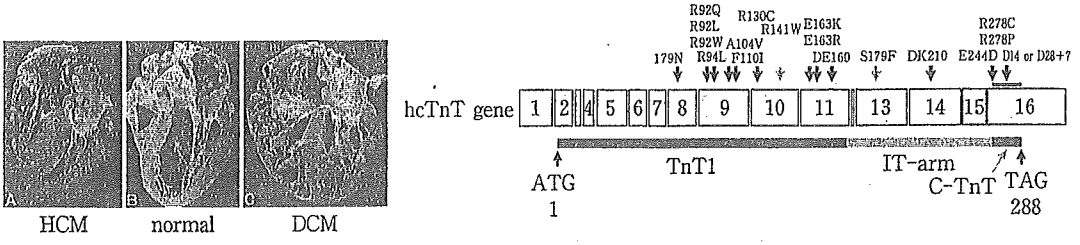

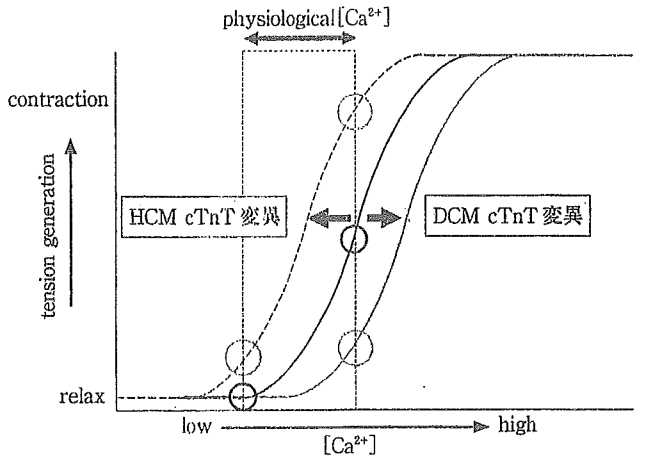

図4 心筋症におけるトロポニンの遺伝子変異と筋カルシウム感受性
心筋症の遺伝子変異はTnT1，C-TnTに多く，筋カルシウム感受性を修飾する．

ルシウムセンシタイザーはphoshodiesteraseの阻害作用も併せてもっており，細胞内cyclic-AMPの増加によって筋小胞体からのカルシウムイオン放出が増加し，ついにはカルシウムoverloadとなる可能性や[7]，構造が類似した他の蛋白と相互作用があるなど，薬剤としての標的特異性が低いことが原因として考えられる．拡張型心筋症例では，少なくとも一部の症例でカルシウム感受性の低下と収縮不全の関連が示唆されている．これらの事実はTnCやTnTを特異的に制御する化合物の設計により，新たな強心剤の開発の可能性を示している．

一方，肥大型心筋症(HCM)ではトロポニンの遺伝子変異によりカルシウム感受性が亢進することが発病に関連する可能性が示唆されている．同患者の遺伝子解析によると，約15%の患者にTnTの遺伝子変異が認められる．大槻らによれば[5]トロポニンがアクチン/トロポミオシンと直接接触する部分(TnT1，C-TnT，TnI調節領域)に変異が多く認められ，コアドメインには変異は少ないという(図4)．変異TnTの交換導入を行った心筋スキンドファイバーを用いた研究で，カルシウムイオン濃度-張力関係の左方シフト，すなわちカルシウム感受性の亢進が認められた．この結果からTnTの変異により，カルシウム感受性が亢進し，収縮増加と弛緩不全という肥大型心筋症に特有の症状が発症するという有力な仮説が生まれる．TnTの変異によるカルシウム感受性亢進のメカニズムを原子構造で解明すると，肥大型心筋症に特異的に作用する薬剤の設計を期待できる．原因となる遺伝子変異ごとに構造が異なる薬剤設計が求められる可能性もある．言い換えれば，心筋トロポニンの変異に基づく肥大型心筋症の治療法の開発はテーラーメード医療のモデルケースとなる可能性がある．

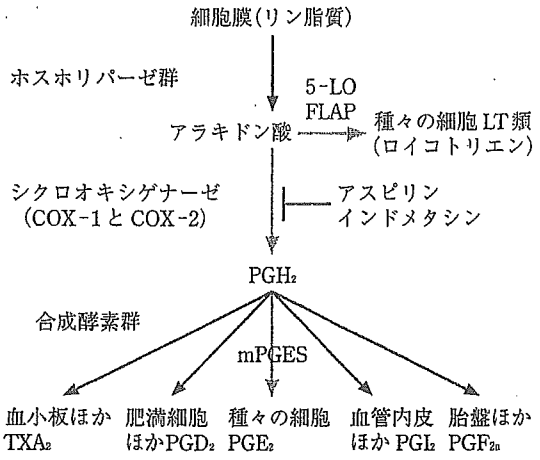

図5 プロスタグランジン産生系

3. 創薬の標的として注目されているプロスタグランジン合成酵素群の構造解析

シクロオキシゲナーゼ(COX)はプロスタグランジン(PG)を生合成する律速酵素として知られている(図5)2種類のアイソザイムが存在する．COX-1はconstitutive enzymeと呼ばれ，ほとんどの細胞で常時発現しており，生体の安定性を維持する役割を果たす．一方，COX-2はinducible enzymeとして，単球，線維芽細胞，滑膜細胞などの炎症にかかわる細胞で発現し，炎症性サイトカインなどによって誘導される．従来の非ステロイド系抗炎症剤は，COX-1とCOX-2の両方を阻害するために炎症巣のPGだけでなく，胃粘膜や腎でのPG(特にPGE_2)産生を抑制し胃や腎の副作用を合併する．そこで，炎症に深く関与していると考えられるCOX-2だけを選択的に阻害する薬剤の開発が進められてきた．このようにして開発されたCOX-2阻害薬は胃潰瘍を起こしにくい鎮痛剤として好んで投薬されていた．しかしながら，2004年末，米政府は，これらのCOX-2選択的阻害薬の3剤を心筋梗塞や脳梗塞の危険性を高める恐れがあるとして，心臓病患者への処方や多量の長期使用を避けるよう勧告した．COX-2の下流に位置するプロスタサイクリン合成酵素の作用も抑制するために，同酵素に由来する抗血栓性作用や血流増加作用が損なわれることが原因ではないかと考えられている[8]．図5に示したようにCOX-2の下流には多くの合成酵素があってそれぞれの作用を有する蛋白を合成している．個々の合成酵素を選択的に阻害する薬剤の開発が次世代の創薬の標的として注目される．PGE_2の産生にかかわるmPGESを阻害する薬物の開発は血管内血栓形成を伴わない理想的な抗炎症剤となる可能性がある．TXA_2産生を阻害する薬剤の開発は血管内血栓形成の予防，局所血流増加作用を通じて脳梗塞，心筋梗塞の予防薬や治療薬として期待できる．PGI_2は既に難病といわれた原発性肺高血圧症の治療に有効であることが知られている．PG関連薬剤の開発は構造に基づく創薬の最大の標的の一つになっており，ナノメディシンプロジェクトでも複数の関連酵素の構造解析に取り組んでいる．

4. ナノメディシンプロジェクトのそのほかの研究

本プロジェクトでは分子構造イメージングに関連して上記のほかに，細胞内イオン環境や，血管新生にかかわる蛋白など幾つかの蛋白構造についても研究を進めている(国立循環器病センター研究所)．国立精神神経センターではin-silicoスクリーニング法によるParkinson病の治療薬探索に蛋白構造情報を応用する研究を進めている．国立医薬品食品衛生研究所では原子間力顕微鏡を用いて蛋白表面の詳細な構造を解析することなどを通じて，医用材料作成に向けた応用研究に取り組んでいる．

一方，分子機能イメージングの領域では，国立循環器病センターの望月らが増殖因子(EGF)刺激に伴うRas分子の活性化をFRET法で可視化できることをNature誌に報告した[9]．ナノメディシンプロジェクト開始後も血管内皮の走化運動にかかわるRap1蛋白の可視化に関する研究などにFRET法による分子イメージングを展開している．国立精神神経センターの研究グループでは分子機能イメージング技術を応用してシナプス機能，プリオン蛋白質の機能の評価に

取り組みProc Natl Acad Sciなどの雑誌に研究成果を報告している[10].

おわりに

本ナノメディシンプロジェクトでは循環器治療の中核施設である国立循環器病センター内に構造生物学ラボを立ち上げ，分子特異的な治療薬の開発を目指している．ナノDDS技術や分子機能イメージング技術に関する研究を併せて推進することで，特異的分子治療薬の分子輸送技術開発と他の分子との相互作用の可視化技術を推進することが可能となる．これにより，分子診断・分子治療・分子評価を包含するテーラーメード医療の基盤形成に貢献したい．

謝辞　本原稿の執筆内容は本研究グループの成果を元にしております．国立循環器病センター研究所若林繁夫分子生理部長およびユーセフ・ベン・アマー同研究員，増田道隆循環器形態部室長，柴田洋之心臓生理部同室員，五十嵐智子同研究員，松原孝宜同研究員，大阪大学月原富武教授，理化学研究所宮野雅司主任研究員に感謝いたします．また，本原稿編集と英文作成に協力していただいた東本弘子女史，松尾千重女史に感謝します．

文　献

1) Patick AK, et al: Activities of the human immunodeficiency virus type 1(HIV-1) protease inhibitor nelfinavir mesylate in combination with reverse transcriptase and protease inhibitors against acute HIV-1 infection in vitro. Antimicrob Agents Chemother 41: 2159-2164, 1997.
2) Drucker BJ, et al: Effects of a selective inhibitor of the Abl tyrosine kinase on the growth of Bcr-Abl positive cells. Nat Med 2: 561-566, 1996.
3) Takeda S, et al: Structure of the core domain of human cardiac troponin in the Ca^{2+} saturated form. Nature 424: 35-41, 2003.
4) 前田雄一郎ほか：トロポニンの結晶構造とカルシウム調節のメカニズム．蛋白質核酸酵素 48: 500-512, 2003.
5) 大槻磐男：筋収縮カルシウム受容調節の分子機構と遺伝性機能障害．日薬理誌 118: 147-158, 2001.
6) Lee JA, et al: Effects of pimobendan, a novel inotropic agent on intracellular calcium and tension in isolated ferret ventricular muscle. Clin Sci 76: 609-618, 1989.
7) Nieminen MS, et al: Executive summary of the guidelines on the diagnosis and treatment of acute heart failure: The task force on acute heart failure of the European society of cardiology. Eur Heart J 26: 384-416, 2005.
8) Mukherjee D, et al: Risk of cardiovascular events associated with selective cox-2 inhibitors. JAMA 286: 954-959, 2001.
9) Mochizuki N, et al: Spatio-temporal images of growth-factor-induced activation of Ras and Rap1. Nature 411: 1065-1068, 2001.
10) Itami C, et al: Brain-derived neurotrophic factor-dependent unmasking of silent synapses in developing mouse barrel cortex. Proc Natl Acad Sci USA 100: 13069-13074, 2003.

Available online at www.sciencedirect.com
SCIENCE DIRECT®
European Journal of Pharmacology 508 (2005) 23–30
ELSEVIER
ejp
www.elsevier.com/locate/ejphar

Characterization of voltage-dependent gating of $P2X_2$ receptor/channel

Ken Nakazawa[a,*], Yasuo Ohno[b]

[a]*Cellular and Molecular Pharmacology Section, Division of Pharmacology, National Institute of Health Sciences, 1-18-1 Kamiyoga, Setagaya, Tokyo 158-8501, Japan*
[b]*Division of Pharmacology, National Institute of Health Sciences, 1-18-1 Kamiyoga, Setagaya, Tokyo 158-8501, Japan*

Received 9 September 2004; received in revised form 29 November 2004; accepted 6 December 2004
Available online 4 January 2005

Abstract

The role of a voltage-dependent gate of recombinant $P2X_2$ receptor/channel was investigated in *Xenopus* oocytes. When a voltage step to −110 mV was applied from a holding potential of −50 mV, a gradual increase was observed in current evoked by 30 μM ATP. Contribution of this voltage-dependent component to total ATP-evoked current was greater when the current was evoked by lower concentrations of ATP. The voltage-dependent gate closed upon depolarization, and half the gates were closed at −80 mV. On the other hand, a potential at which half the gates opened was about −30 mV or more positive, which was determined using a series of hyperpolarization steps. The results of the present study suggest that the voltage-dependent gate behavior of $P2X_2$ receptor is not due to simple activation and deactivation of a single gate, but rather due to transition from a low to a high ATP affinity state.

Keywords: P2X receptor; Voltage dependence; Gate; Kinetics; Ligand affinity

1. Introduction

Extracellular ATP is considered a neurotransmitter, and its fast neurotransmission is mediated through ion channel-forming P2X receptors (see reviews, Ralevic and Burnstock, 1998; Khakh, 2001; North, 2002). To date, at least seven subclasses of P2X receptor ($P2X_{1-7}$) have been cloned, which form homo- or heteromeric receptors that act as functional ion channels (North and Surprenant, 2000). Each subclass consists of two transmembrane domains (TM1 and TM2) and one long extracellular domain (E1) between them. Both TM1 (Jiang et al., 2001; Haines et al., 2001) and TM2 (Rassendren et al., 1997; Egan et al., 1998; Migita et al., 2001) contribute to formation of the channel pore. P2X receptor/channels are permeable to cations, but demonstrate poor cation selectivity. The channels are gated by ATP molecules, and the narrowest part of the channel pore opens when activated (Rassendren et al., 1997). The ATP-binding site for gating is partly attributable to basic amino acid residues near the outer mouth of the channel pore formed by TM1 and TM2 (Ennion et al., 2000; Jiang et al., 2000), and the possibility that aromatic residues in E1 contribute to the binding site has also been suggested (Nakazawa et al., 2002; Roberts and Evans, 2004).

In addition to ATP, other factors are known to modulate channel activity. Zn^{2+} and acidic conditions facilitate ATP-mediated gating by increasing ATP sensitivity of $P2X_2$ receptor (Clyne et al., 2002). Neurotransmitters, including dopamine, and related compounds also facilitate ATP-mediated gating (Nakazawa et al., 1997a). Membrane potential may also play a role. It has been reported that ionic current activated by ATP is enhanced by hyperpolarization in pheochromocytoma PC12 cells (Nakazawa et al., 1997b). We observed similar voltage-dependent gating of recombinant $P2X_2$ receptor/channel, which was originally cloned from PC12 cells (Brake et al., 1994), and qualitatively analyzed its properties in the present study.

2. Methods

Recordings of ionic current through recombinant $P2X_2$ receptor/channels were performed according to our previous

* Corresponding author. Tel.: +81 3 3700 9704; fax: +81 3 3707 6950.
E-mail address: nakazawa@nihs.go.jp (K. Nakazawa).

0014-2999/$ - see front matter © 2004 Elsevier B.V. All rights reserved.
doi:10.1016/j.ejphar.2004.12.005

report (Nakazawa and Ohno, 1997). Briefly, the cloned rat $P2X_2$ receptor (Brake et al., 1994) was expressed in *Xenopus* oocytes by injecting in vitro transcribed cRNA. After 4 days of incubation at 18 °C, the membrane current of the oocytes was recorded. Oocytes were bathed in ND96 solution containing (in mM) NaCl 96, KCl 2, $CaCl_2$ 1.8, $MgCl_2$ 1, HEPES 5 (pH 7.5 with NaOH). In some experiments, oocytes were bathed in solution containing 10.8 mM $BaCl_2$ instead of 1.8 mM $CaCl_2$. When achieving a low extracellular chloride concentration, 96 mM Na-acetate was added instead of 96 mM NaCl. ATP (adenosine 5′-triphosphate disodium salt; Sigma, St. Louis, MO, U.S.A.) was applied by superfusion for approximately 10 s at regular 2-min intervals. Membrane current was recorded using the standard two-electrode voltage-clamp techniques, and electrical signals were stored on a data recorder (PC204Ax; SONY, Tokyo, Japan) for off-line analysis. Curve fittings to data were made using Microsoft' Excel X.

3. Results

3.1. Voltage-dependent component of ATP-evoked current

Fig. 1A compares membrane currents in the absence and presence of 30 μM ATP in a $P2X_2$ receptor-expressing oocyte. The oocyte was held at −50 mV and stepped to −110 mV for 200 ms. In the presence of ATP, inward current at −110 mV did not instantaneously reach steady-state, but gradually increased: a biphasic increase in current was observed with a voltage-independent component ("a" in Fig. 1A) and a voltage-dependent component ("b" in Fig. 1A). When the voltage was returned to −50 mV, a gradually declining inward "tail" current was observed ("c" in Fig. 1A). The voltage-dependent component of the inward current at −110 mV was observed to follow first-order kinetics with a time constant of 40 ms (Fig. 1B).

Fig. 2A demonstrates an increased magnitude of the voltage-dependent component when activated from a less negative holding potential. The voltage-dependent component was larger when the step to −110 mV was applied from −10 mV ("a" in Fig. 2A) than when it was applied from −70 mV ("b" in Fig. 2A). This dependence of the voltage-dependent component on holding potentials is illustrated in Fig. 2B. It is worth noting that Ca^{2+}-activated currents exist in *Xenopus* oocytes (Weber, 1999; Zhang and Hamill, 2000). Since P2X receptor/channels are Ca^{2+}-permeable (Khakh, 2001), a secondarily activated Ca^{2+}-induced current might contribute to the observed voltage-dependent changes. This does not, however, appear to be the case since a similar dependence on holding potentials was observed when extracellular Ca^{2+} was replaced with 10.8 mM Ba^{2+}. Time constants for the activation of the voltage-dependent component were obtained as shown in Fig. 1B, and the mean values were plotted against holding potentials

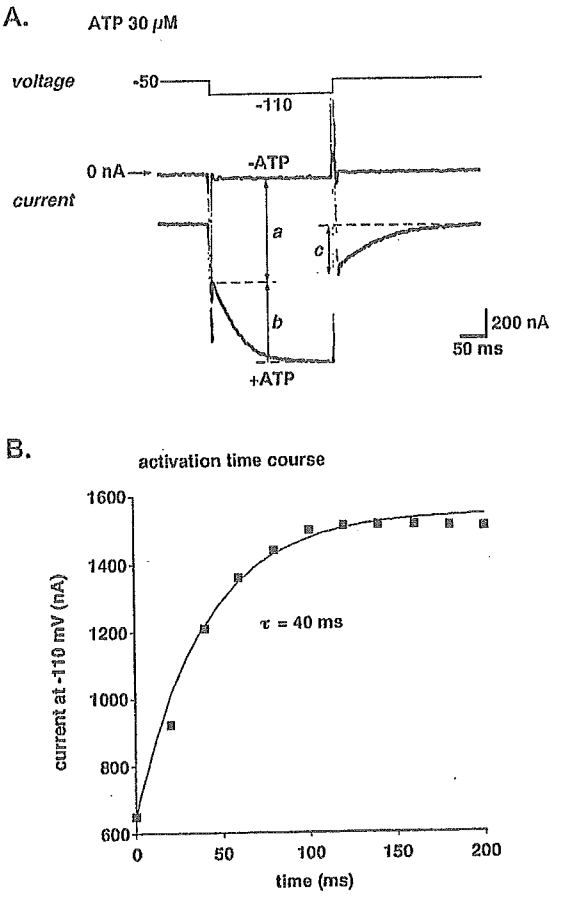

Fig. 1. (A) Current traces of an oocyte stepped to −110 mV from a holding potential of −50 mV in the absence (−ATP) or presence (+ATP) of 30 μM ATP. The current evoked by ATP is represented by the difference between the two traces. Upon hyperpolarization, a gradual increase in current was observed in the presence of ATP, suggesting activation of a voltage-dependent gate (denoted by "b"). The current denoted by "c" represents a gradually declining "tail current" that was observed when the voltage was returned to −50 mV. (B) Time course of activation of the voltage-dependent component. Current amplitude of the voltage-dependent component represented by "b" in panel A was plotted against time after the onset of hyperpolarization at −110 mV. The voltage-dependent component could be made to fit a curve with a time constant of 40 ms.

(Fig. 2C). While the current amplitude demonstrated voltage dependence (Fig. 2B), voltage did not have an effect on time course of the activation.

3.2. Effect of ATP concentrations

Fig. 3A shows the voltage-dependent component of the current activated by 10 μM or 300 μM of ATP in a single oocyte. The relative size of the voltage-dependent component involved in total ATP-evoked current became smaller when the current was evoked by greater concentrations of ATP (Fig. 3A and B). A similar dependence on ATP concentration was observed for the current evoked in the presence of 10.8 mM Ba^{2+} instead of 1.8 mM Ca^{2+} (Fig. 3B). Dependence on ATP concentrations was also found for activation time constants for the voltage-

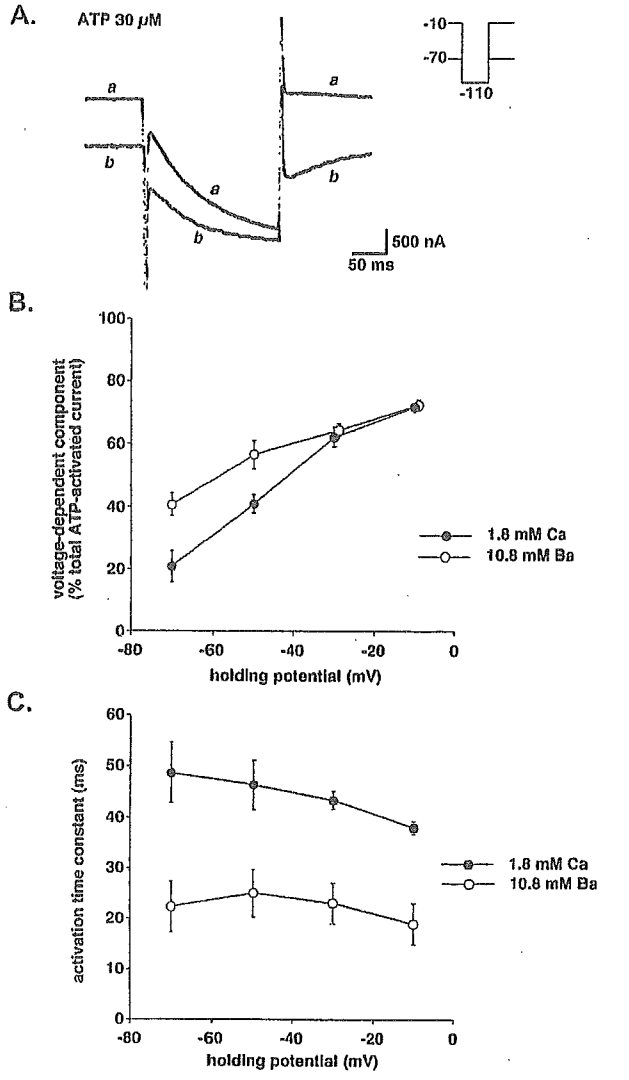

Fig. 2. Effect of holding potential on current. Current was evoked by 30 μM ATP. (A) Voltage-dependent current at −110 mV when stepped from a holding potential of −10 mV ("a") or −70 mV ("b"). (B) Effect of holding potential on voltage-dependent current. The amplitude of the voltage-dependent current was measured as described in Fig. 1A. Mean values obtained from 4 oocytes in a standard extracellular solution containing 1.8 mM Ca^{2+} (●) and an extracellular solution containing 10.8 mM Ba^{2+} (instead of Ca^{2+}; O) were plotted. Bars represent the S.E.M. (C) Time course of activation of the voltage-dependent component. Time constants were determined as shown in Fig. 1B, and mean values obtained from 4 oocytes were plotted against holding potentials. Bars represent the S.E.M.

dependent component; the time constants were larger for 10 μM ATP than 30 μM ATP (Fig. 3C).

3.3. Activation and deactivation kinetics

Cl^- currents are observed in *Xenopus* oocytes (Weber, 1999; Zhang and Hamill, 2000). In the following experiments, current measurements were made using an extracellular solution containing 96 mM Na-aspartate instead of NaCl in order to facilitate the analysis of the voltage-dependent component of ATP-evoked current by reducing Cl^- currents. In doing so, there was an obvious reduction in outward current upon depolarization, resulting in better voltage-clamp conditions. Using this extracellular solution, the EC_{50} value for ATP-activated current measured at −50 mV was about 40 μM, which was lower than the value obtained with the standard extracellular solution containing 96 mM NaCl (about 100 μM; Nakazawa and Ohno, 2004). Fig. 4 illustrates

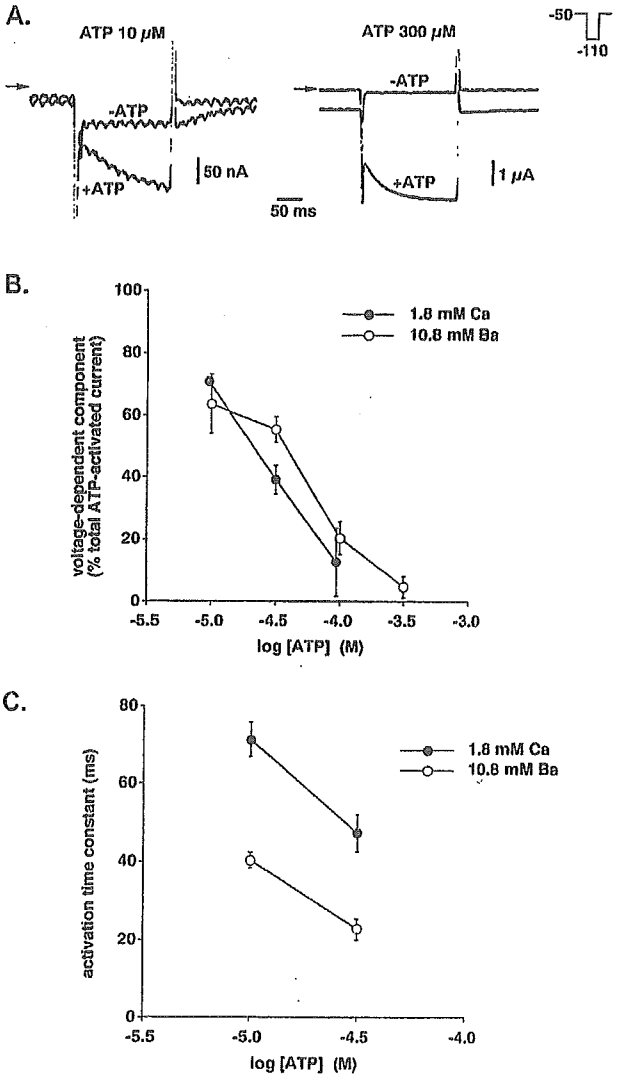

Fig. 3. Effect of ATP concentration. The voltage-dependent current was activated by hyperpolarization (−110 mV) from a holding potential of −50 mV. (A) Voltage-dependent current activated by 10 μM or 30 μM ATP. Current traces in the absence (−ATP) or presence (+ATP) of ATP are superimposed in each panel. (B) Contribution of the voltage-dependent current to total ATP-evoked current using different ATP concentrations. Mean values obtained from 4 oocytes in a standard extracellular solution containing 1.8 mM Ca^{2+} (●) and an extracelllular solution containing 10.8 mM Ba^{2+} (instead of Ca^{2+}; O) were plotted. Bars represent the S.E.M. (C) Time course of activation of the voltage-dependent components. Time constants were determined as shown in Fig. 1B, and mean values obtained from 4 oocytes were plotted against holding potentials. Bars represent the S.E.M.

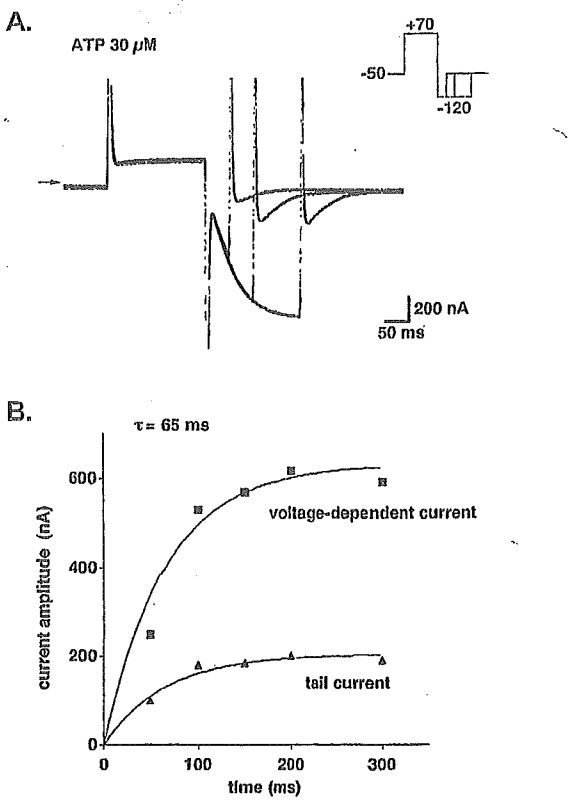

Fig. 4. Activation and tail current. (A) Gradual increase in magnitude of the tail current with increasing voltage-dependent current. Current traces obtained upon exposure to hyperpolarizing pulses (−120 mV) of different durations are superimposed. (B) Time course of activation of the voltage-dependent (■) and tail (▲) currents. Current amplitude was plotted against duration of hyperpolarization (also shown in panel A). The results of both time course activation experiments fit curves with a single time constant of 65 ms.

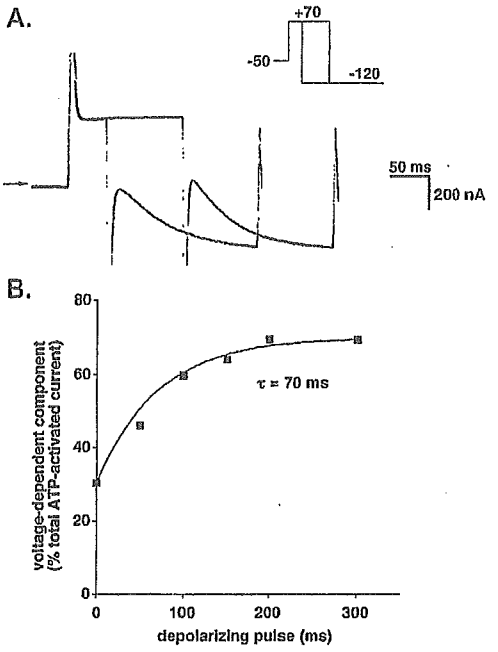

Fig. 5. Deactivation of the voltage-dependent component. (A) Current traces obtained using depolarizing pulses (+70 mV) of two different durations. The amplitude of the voltage-dependent component increased when the duration was prolonged. (B) Time course of deactivation of the voltage-dependent component. Current amplitude was plotted against duration of the depolarizing pulses (also shown in panel A).

the relation between activation kinetics of the voltage-dependent component and time course of tail current. As shown in Fig. 4A, oocytes were stepped to 70 mV and then to −120 mV to induce the voltage-dependent component. When hyperpolarization at −120 mV was terminated after various periods, a gradual increase in amplitude of the tail current was observed with increased duration of hyperpolarization at −120 mV. Time courses of both the voltage-dependent component and tail current could be fitted with curves with a single time constant (65 ms in this case; Fig. 4B). Similar fitting with single time constants were made for 4 oocytes tested, and the mean time constant±S.E.M. was 66.3±2.4 ms.

With increased duration of the +70 mV depolarizing pulse, increased amplitude of the voltage-dependent component was observed at −120 mV (Fig. 5A). This may reflect "deactivation" of the voltage-dependent component (Scheme 1):, where A is ATP, and R and R* are closed and open states, respectively, of the voltage-dependent component of $P2X_2$ receptor/channel. The deactivation time course could be fitted with a time constant of 70 ms in this case (Fig. 5B; mean±S.E.M., 71.3±1.3 ms; n=4).

3.4. Voltage dependence of activation and deactivation

As shown in Fig. 1, contribution of the voltage-dependent component to total ATP-evoked current was influenced by the holding potential prior to hyperpolarization. This was further examined by testing a number of prepulses at various potentials prior to hyperpolarization (Fig. 6A). As the prepulse became more depolarized, a greater contribution of the voltage-dependent component to total ATP-evoked current was observed, and this contribution became maximal near 0 mV (Fig. 6B). Thus, the voltage-dependent gate must be completely closed at potentials equal to or more positive than 0 mV. The data were fitted with a curve in accordance with the following model of "deactivation":

$$d_\infty = 1/\{1 + \exp[(E_{1/2} - E_m)/k]\}, \quad (1)$$

where d_∞ represents the relative proportion of closed gates at steady state, $E_{1/2}$ is the voltage at which the half-maximal closing occurs, E_m is the membrane potential, and

$$A{\cdot}R \underset{\text{(deactivation)}}{\overset{\text{(activation)}}{\rightleftharpoons}} A{\cdot}R^*$$

Scheme 1.

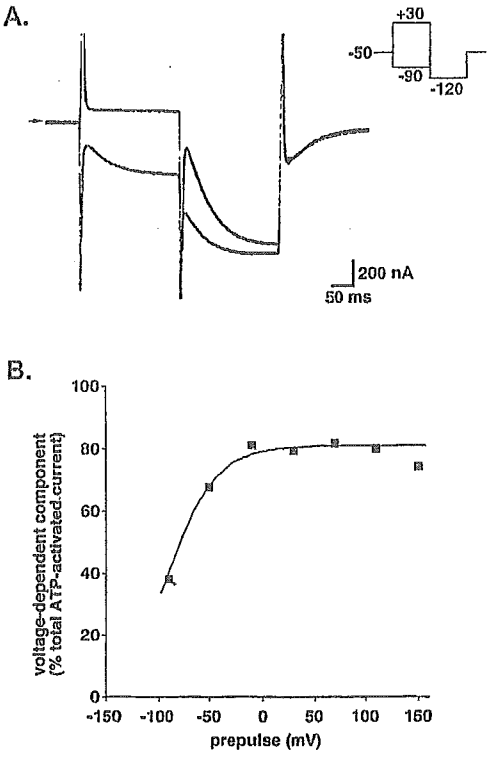

Fig. 6. Prepulse experiment. An ATP concentration of 30 μM was used. (A) Current traces obtained using prepulses of +30 mV ("a") or −90 mV ("b") prior to hyperpolarization at −120 mV. (B) Effect of prepulses. The relative contribution of the voltage-dependent current to total ATP-evoked current at −120 mV was plotted against each prepulse voltage. Some of this data is also shown in panel A.

k is a slope factor reflecting an energy barrier (Hodgkin and Huxley, 1952; Hille, 1992a). As shown in Fig. 6B, potential at which half the gates closed was estimated to be −90 mV in this case (mean±S.E.M., −78.8±5.2 mV; n=4).

The voltage dependence of activation was also examined. As shown in Fig. 7A, the channels responsible for the voltage-dependent component was sufficiently "deactivated" by applying a prepulse of +100 mV, and they were then activated at various hyperpolarization potentials. Contribution of the voltage-dependent component to total ATP-evoked current decreased as the hyperpolarization became more negative up to −45 mV in the case shown in Fig. 7B. Potentials exceeding −45 mV could not be examined since the resultant ATP-evoked current was not large enough to analyze. The data were fitted in accordance with the following model of "activation":

$$a_\infty = 1/\{1+\exp[(E_{1/2}-E_m)/k]\}, \quad (2)$$

where a_∞ represents the degree of gate opening at steady state. The other parameters are the same as those described above. The data obtained using Eq. (2) (Fig. 7B) could be fitted with a curve indicating that half of the gates were open at a potential of −30 mV.

The above data suggest that activation of the voltage-dependent gate occurs at more positive potentials than gate deactivation. To further investigate this, the fraction of the gates that escaped deactivation ($1-d_\infty$) was calculated from the data obtained during deactivation experiments. The deactivation data was then plotted alongside data obtained from activation experiments (Fig. 7C). These data suggest that the activation potential is 50 mV more positive than the deactivation potential.

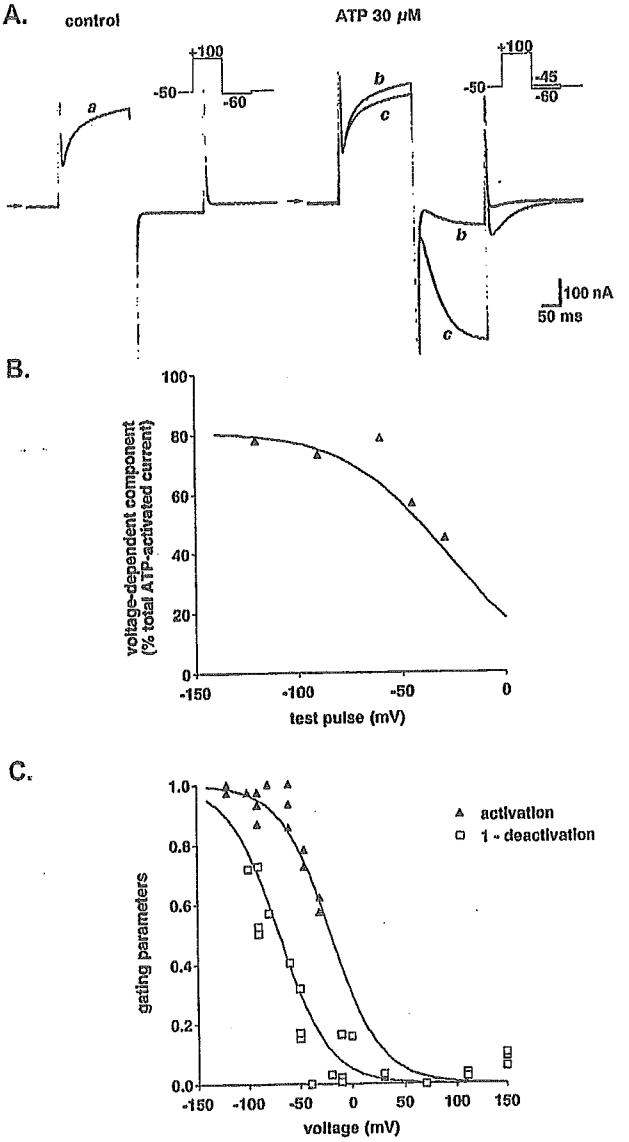

Fig. 7. Effect of hyperpolarization on voltage-dependent current. (A) Current traces before (control) and during the application of 30 μM ATP. In the panel on the right, two current traces obtained following hyperpolarization at −45 mV ("b") and −60 mV ("c") are superimposed. (B) Contribution of voltage-dependent current to total ATP-evoked current at various hyperpolarization potentials. Some of these data are shown in panel A. (C) Comparison of activation and deactivation. Parameters describing activation and deactivation were determined as described in the text. Each data point represents data obtained from individual oocytes.

4. Discussion

4.1. Schematic model of voltage-dependent gating

Recombinant $P2X_2$ receptor/channels expressed in *Xenopus* oocytes exhibited voltage-dependent gating properties similar to those of the channels in PC12 cells (Nakazawa et al., 1997b). The following similarities were observed: (1) the gate opens at negative potentials, (2) activation follows a time course with a time constant of 40 to 70 ms, and (3) gating depends on ATP concentrations. Thus, voltage-dependent gating in PC12 cells may be due to intrinsic expression of $P2X_2$ receptor/channels. We depict here a model that has been proposed to explain voltage-dependent gating of the channels in PC12 cells (Scheme 2):, where A is ATP, R_L and R_H represent closed states, and R* represents the open state (Nakazawa et al., 1997b). In this model, voltage-dependent gating is explained by transition between low and high ATP-affinity states. Upon hyperpolarization, there is a shift from the R_L to the R_H conformation. ATP preferentially binds to channels in the R_H state ($A \cdot R_H$), after which the channels open ($A \cdot R_H$*). Binding of ATP is the rate-limiting step since activation kinetics were observed to depend on ATP concentrations in the present study (Fig. 3C). The following rate constants have been proposed (Scheme 3): where k_{+1} parallels the concentration of ATP ($k_{+1}=k'_{+1}$[ATP]), and K_d is given by k_{-1}/k'_{+1} (Hille, 1992b). In the present experiment, an activation time constant of 65 ms was observed in the presence of 30 μM of ATP (Fig. 4), which is equivalent to a rate constant of 15 s^{-1}. Using these values, $k'_{+1}=k_{+1}/[ATP]=15\ s^{-1}/(30\ \mu M)=5\times10^5\ M^{-1}\ s^{-1}$. An inactivation time constant of 70 ms was observed in the presence of 30 μM of ATP (Fig. 5), which is equivalent to a rate constant of 14 s^{-1}. Thus, K_d was calculated to be $k_{-1}/k'_{-1}=14\ s^{-1}/(5\times10^5\ M^{-1}\ s^{-1})=28\ \mu M$, which is slightly less than the EC_{50} value obtained at −50 mV (about 40 μM). This estimation is in accordance with the finding that the voltage-dependent component is not completely activated at −50 mV (Fig. 7C). It is difficult to quantify the low-affinity ATP binding state since the relationship between concentration and response needs to be assessed at highly positive potentials, while $P2X_2$ receptor/channels permit only small current due to their inward-rectifying

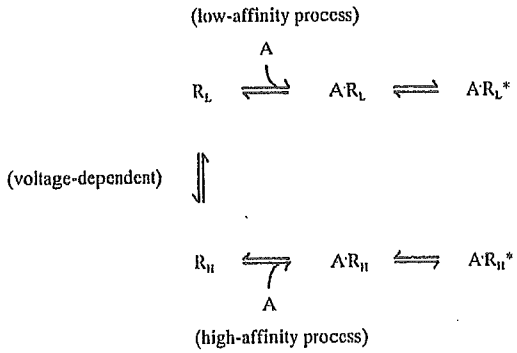

Scheme 2.

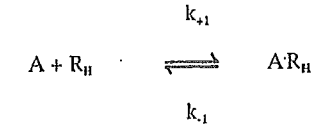

Scheme 3.

nature. We estimate here the low affinity from simple theoretical concentration–response curves. Fig. 8 shows two concentration–response curves. One demonstrates an EC_{50} of 30 μM, corresponding to a high-affinity state. If the other low-affinity state demonstrates an EC_{50} of 100 μM, more $P2X_2$ receptor/channels were in the high-affinity state in the presence of 10 μM ATP, and more were in the low-affinity state in the presence of 300 μM ATP. This is consistent with the greater observed contribution of the voltage-dependent component to total ATP-evoked current in the presence of 10 μM, while little was observed in the presence of 300 μM ATP (Fig. 3). Thus, the low-affinity state may be lower than the high-affinity state by threefold or larger.

The idea of the transition of $P2X_2$ receptor/channels between low- and high-affinity states might explain the "non-voltage-dependent" component of ATP-evoked current. For example, the current evoked by 30 μM ATP was not completely observed as voltage-dependent component even when activated at very negative potentials (Fig. 7B) or following deactivation at very positive potentials (Fig. 6B). This "non-voltage-dependent current" (about 20% of the total ATP-evoked current) might result from the activation of $P2X_2$ receptor/channels in the low-affinity state prior to voltage-dependent activation.

The voltage dependence of activation and deactivation differed, with deactivation occurring at more negative potentials (Fig. 7C). This indicates that the activation and the deactivation do not arise from a simple reversible "back-and-forth" process, rather, two voltage-dependent processes

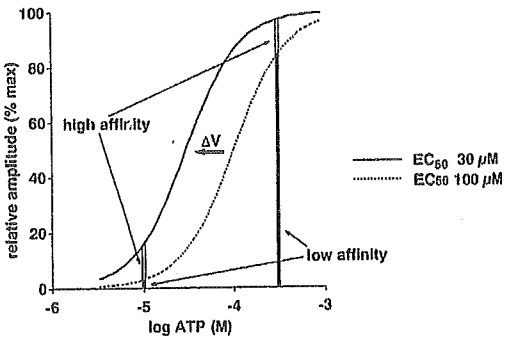

Fig. 8. Voltage-dependent change in sensitivity to ATP might explain dependence of the voltage-dependent current on ATP concentration. Low-affinity (EC_{50}=100 μM) and high-affinity (EC_{50}=30 μM) states of the receptor are thought to exist (Hill coefficient; 1.5). Each receptor shifts from a low-affinity to a high-affinity state upon hyperpolarization (ΔV). With 10 μM ATP, only a small proportion of the receptors, many of which were in the low-affinity state, were activated prior to hyperpolarization, but many more were activated upon induction of the high-affinity state by hyperpolarization. In the presence of 300 μM ATP, a larger proportion of the receptors were activated even in the low-affinity state, and induction of the high-affinity state caused only a marginal increase in activated receptors.

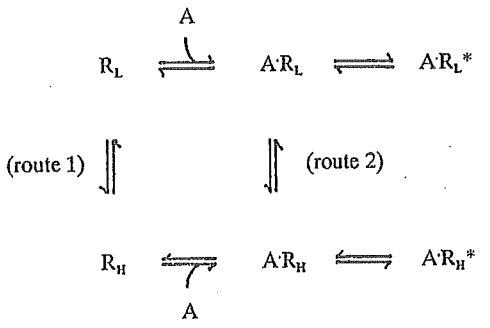

Scheme 4.

may be involved. We propose the following modification to Scheme 2.

This model (Scheme 4) involves two voltage-dependent processes, one resulting in activation through "route 1", and the other resulting in deactivation through "route 2". Such model would explain the observed difference in voltage dependence between activation and deactivation. However, we would expect this model to result in more difficult to interpret data than we did above based on Schemes 2 and 3.

4.2. Relevance of voltage-dependent gating

$P2X_2$ receptor is expressed in a number of neurons (e.g., Atkinson et al., 2000; Rubio and Soto, 2001). $P2X_2$ receptor/channel is permeable to Ca^{2+} (Egan and Khakh, 2004), and Ca^{2+} influx through the channel may influence cellular activity, although its exact role remains to be clarified. The voltage-dependent gating reported here may be relevant to the Ca^{2+} influx from the following consideration. Na^+ current (I_{Na}) and Ca^{2+} current (I_{Ca}) permeating through $P2X_2$ receptor/channel are:

$$I_{Na} = -P_{Na}\frac{E_m F^2}{RT}\frac{[Na]_o}{1-\exp(-EF/RT)} \quad (3)$$

$$I_{Ca} = -4P_{Ca}\frac{E_m F^2}{RT}\frac{[Ca]_o \exp(-2EF/RT)}{1-\exp(-2EF/RT)}, \quad (4)$$

where P_{Na} and P_{Ca} represent the permeability of Na^+ and Ca^{2+}, respectively, E_m represents the membrane potential, and F, R, and T are their usual physicochemical meanings (Fatt and Ginsborg, 1958; Nakazawa et al., 1989). The ratio of I_{Na} to I_{Ca} is thus:

$$\frac{I_{Ca}}{I_{Na}} = \frac{4P_{Ca}[Ca]_o}{P_{Na}[Na]_o}\frac{1}{\exp(E_m F/RT)[\exp(E_m F/RT)+1]} \quad (5)$$

This equation indicates that the ratio of I_{Ca}/I_{Na} is larger at more negative potentials. The ratio calculated at −90 mV is about 13-fold larger than that calculated at −30 mV. Thus, channel opening at negative potentials favors Ca^{2+} over Na^+ influx. Thus, voltage-dependent gating may facilitate cellular Ca^{2+}-dependent responses when cells are hyperpolarized. This may occur when efflux through K^+ channels outpaces depolarization afforded by opening of $P2X_2$ receptor/channels.

4.3. Conclusion

The results of the present study suggested that $P2X_2$ receptor exhibits voltage-dependent gating, and that this is not due to simple activation and deactivation of a single gate, but rather, due to a transition from a low ATP affinity to a high ATP affinity state. This may favor Ca^{2+} influx at negative potentials, although further studies are required to clarify the physiological significance of voltage-dependent gating of $P2X_2$ receptor.

Acknowledgements

This work was supported, in part, by a Health and Labour Science Research Grant for Research on Advanced Medical Technology from the Ministry of Health, Labour and Welfare, Japan, as well as a grant-in-aid for scientific research from the Ministry of Education, Science, Sports and Culture, Japan (KAKENHI 13672319) awarded to K.N.

References

Atkinson, L., Batten, T.F., Deuchars, J., 2000. $P2X_2$ receptor immunoreactivity in the dorsal vagal complex and area postrema of the rat. Neuroscience 99, 683–696.

Brake, A.J., Wagenbach, M.J., Julius, D., 1994. New structural motif for ligand-gated ion channels defined by an ionotropic ATP receptor. Nature 371, 519–523.

Clyne, J.D., LaPointe, L.D., Hume, R.I., 2002. The role of histidine residues in modulation of the rat $P2X_2$ purinoceptor by zinc and pH. J. Physiol. 539, 347–359.

Egan, T., Khakh, B.S., 2004. Contribution of calcium ions to P2X channel responses. J. Neurosci. 24, 3413–3420.

Egan, T.M., Haines, W.R., Voigt, M.M., 1998. A domain contributing to the ion channel of ATP-gated $P2X_2$ receptors identified by the substituted cysteine accessibility method. J. Neurosci. 18, 2350–2359.

Ennion, S., Hagan, S., Evans, R.J., 2000. The role of positively charged amino acids in ATP recognition by human $P2X_1$ receptors. J. Biol. Chem. 275, 29361–29367.

Fatt, P., Ginsborg, B.L., 1958. The ionic requirements for the production of action potentials in crustacean muscle fibres. J. Physiol. 142, 516–543.

Haines, W.R., Migita, K., Cox, J.A., Egan, T.M., Voigt, M.M., 2001. The first transmembrane domain of the P2X receptor subunit participates in the agonist-induced gating of the channel. J. Biol. Chem. 276, 32793–32798.

Hille, B., 1992a. Classical biophysics of the squid giant axon. Ionic channels of excitable membranes, Second Edition. Sinauer, Sunderland, MA, pp. 23–58.

Hille, B., 1992b. Ligand-gated channels of fast chemical synapses. Ionic channels of excitable membranes, Second Edition. Sinauer, Sunderland, MA, pp. 140–169.

Hodgkin, A.L., Huxley, A.F., 1952. The dual effect of membrane potential on sodium conductance in the giant axon of *Loligo*. J. Physiol. 116, 497–506.

Jiang, L.H., Rassendren, F., Surprenant, A., North, R.A., 2000. Identification of amino acid residues contributing to the ATP-binding site of a purinergic P2X receptor. J. Biol. Chem. 275, 34190–34196.

Jiang, L.H., Rassendren, F., Spelta, V., Surprenant, A., North, R.A., 2001. Amino acid residues involved in gating identified in the first membrane-spanning domain of the rat $P2X_2$ receptor. J. Biol. Chem. 276, 14902–14908.

Khakh, B.S., 2001. Molecular physiology of P2X receptors and ATP signalling at synapses. Nat. Rev. 2, 165–174.

Migita, K., Haines, W.R., Voigt, M.M., Egan, T.M., 2001. Polar residues of the second transmembrane domain influence cation permeability of the ATP-gated $P2X_2$ receptor. J. Biol. Chem. 276, 30934–30941.

Nakazawa, K., Ohno, Y., 1997. Effects of neuroamines and divalent cations on cloned and mutated ATP-gated channels. Eur. J. Pharmacol. 325, 101–108.

Nakazawa, K., Fujimori, K., Takanaka, A., Inoue, K., 1989. An ATP-activated conductance in pheochromocytoma cells and its suppression by extracellular calcium. J. Physiol. 428, 257–272.

Nakazawa, K., Liu, M., Inoue, K., Ohno, Y., 1997a. pH dependence of facilitation by neurotransmitters and divalent cations of $P2X_2$ purinoceptor/channels. Eur. J. Pharmacol. 337, 309–314.

Nakazawa, K., Liu, M., Inoue, K., Ohno, Y., 1997b. Voltage-dependent gating of ATP-activated channels in PC12 cells. J. Neurophysiol. 78, 884–890.

Nakazawa, K., Ojima, H., Ohno, Y., 2002. A highly conserved tryptophane residue indispensable for cloned rat neuronal P2X receptor activation. Neurosci. Lett. 324, 141–144.

North, R.A., 2002. Molecular physiology of P2X receptors. Physiol. Rev. 82, 1013–1067.

North, R.A., Surprenant, A., 2000. Pharmacology of cloned P2X receptors. Annu. Rev. Pharmacol. Toxicol. 40, 563–580.

Ralevic, V., Burnstock, G., 1998. Receptors for purines and pyrimidines. Pharmacol. Rev. 50, 413–492.

Rassendren, F., Buell, G., Newbolt, A., North, R.A., Surprenant, A., 1997. Identification of amino acid residues contributing to the pore of a P2X receptor. EMBO J. 16, 3446–3454.

Roberts, J.A., Evans, R.J., 2004. ATP binding at human $P2X_1$ receptors. Contribution of aromatic and basic amino acids revealed using mutagenesis and partial agonists. J. Biol. Chem. 279, 9043–9055.

Rubio, M., Soto, F., 2001. Distinct localization of P2X receptors at excitatory postsynaptic specializations. J. Neurosci. 21, 641–653.

Weber, W.-M., 1999. Ion currents of *Xenopus laevis* oocytes: state of the art. Biochim. Biophys. Acta 1421, 213–233.

Zhang, Y., Hamill, O.P., 2000. Calcium, voltage- and osmotic stress sensitive currents in *Xenopus* oocytes and their relationship to single mechanically gated channels. J. Physiol. 523, 83–99.

Available online at www.sciencedirect.com

SCIENCE DIRECT®

European Journal of Pharmacology 518 (2005) 107 – 110

www.elsevier.com/locate/ejphar

Short communication

Purification and aqueous phase atomic force microscopic observation of recombinant $P2X_2$ receptor

Ken Nakazawa [a,*], Yoko Yamakoshi [b,1], Toshie Tsuchiya [c], Yasuo Ohno [a]

[a] *Division of Pharmacology, National Institute of Health Sciences, 1-18-1 Kamiyoga, Setagaya, Tokyo 158-8501, Japan*
[b] *Division of Organic Chemistry, National Institute of Health Sciences, 1-18-1 Kamiyoga, Setagaya, Tokyo 158-8501, Japan*
[c] *Division of Medical Devices, National Institute of Health Sciences, 1-18-1 Kamiyoga, Setagaya, Tokyo 158-8501, Japan*

Received 4 April 2005; received in revised form 14 June 2005; accepted 20 June 2005
Available online 28 July 2005

Abstract

Recombinant $P2X_2$ receptor was observed by atomic force microscope in the aqueous phase. The $P2X_2$ receptor was expressed in an insect cell line, and recombinant proteins were prepared under native conditions. The membrane fractions were extracted, and histidine-tagged receptor protein was purified from the fractions by column chromatography. When the purified protein fraction was diluted with water and served for atomic force microscopy, dispersed particles of about 3 nm in height were observed. In the presence of 1 mM ATP, the assembly-like images of the particles were obtained. More densely assembled images of the particles were achieved when the protein was dissolved in a Tris buffer containing 1 mM ATP. Under this condition, imaging of the surface of the particles exhibited a circular structure with a diameter of about 10 nm having a pore-like structure. These results suggest that atomic force microscopy provides structural information about $P2X_2$ receptor in aqueous phase.

Keywords: P2X receptor; Atomic force microscopy; Protein structure; ATP

1. Introduction

P2X receptors are ion channel forming membrane proteins that are activated by extracellular ATP, and their physiological roles have been shown in various tissues including the central nervous system (see reviews, Khakh, 2001; North, 2002; Vial et al., 2004). This ion channel/receptor family consists of 7 subclasses ($P2X_1$ to $P2X_7$), and is believed to have molecular structures distinct from so-called "ligand-gated channel super family" including nicotinic acetylcholine receptor/channels and ionotropic glutamate receptor channels. Structural analyses such as the X-ray crystal analysis have not been made for P2X receptor/channel family. In addition, because of their distinct structures, estimation from homology modeling based on known three-dimensional structures of other proteins is difficult. Thus, information concerning the structure and morphology of P2X receptor is lacking. Atomic force microscopy is an approach for structural analysis that allows the analysis of a small amount (nanogram to microgram) of uncrystalized protein. Atomic microscopy enables the observation of both individual and assembled protein molecules in the aqueous phase, which may reveal dynamic forms of biologically active proteins (Müller and Engel, 2002). Recently, Barrera et al. (2005) reported atomic force microscopy imaging of dried P2X receptor protein. In the present study, we have prepared $P2X_2$ receptor protein from an insect cell line expression system, and made atomic force microscopy imaging in aqueous phase. The imaging has revealed that $P2X_2$ receptor is a pore-forming protein for the first time.

* Corresponding author. Tel.: +81 3 3700 9704; fax: +81 3 3707 6950.
E-mail address: nakazawa@nihs.go.jp (K. Nakazawa).
[1] Present address: Center for Polymers and Organic Solids, Department of Chemistry and Biochemistry, University of California, Santa Barbara, CA 93106-9510, USA.

0014-2999/$ - see front matter © 2005 Elsevier B.V. All rights reserved.
doi:10.1016/j.ejphar.2005.06.018